

# Tunneling conductivity features of the new reconstructed phases on the GaN (0001) surface

N. S. Maslova<sup>+</sup>, V. I. Panov<sup>+</sup>, K. Wu<sup>\*</sup>, Q. Z. Xue<sup>\*</sup>, T. Nagao<sup>\*</sup>, A. I. Oreshkin<sup>+\*1)</sup>

<sup>+</sup>Physical department, Moscow State University, 119992 Moscow, Russia

<sup>\*</sup>Institute for Materials Research, Tohoku University, Sendai 980-8577, Japan

Submitted 6 October 2003

Two new Au-induced reconstructed phases on the GaN (0001) surface have been found out and investigated by STM/STS method. Ring-like and  $c(2\times 12)$  surface nanostructures were observed on STM images. The commensurate  $c(2\times 12)$  structure ( $\alpha$ -phase) according to our spectroscopic measurements demonstrates properties of 1D system whereas the incommensurate  $\beta$ -phase looks similar to disordered 2D system.

PACS: 61.16.-d, 71.70.Gm

GaN and its related alloys have become a very attractive subject in past several years for some reasons. On one hand GaN is of interest for practical application in a short-wave optical range for creation optoelectronic devices and on the other hand the unique incommensurate fluid-like structure of the surface stimulates interest such as the transition from incommensurate to commensurate phases by the adsorption of metals, and the influence of the fluid structure on the growth of metals on the GaN surface. During last several years we were able to observe grate developments in both high quality material growth [1] and device fabrications [2–4]. At the same time some fundamental questions, i.e., adsorption mechanism, growth mode, possible metal-induced reconstructions and their properties are still not clear. Wurtzite GaN is a polar semiconductor with two basal planes, i.e., the Ga-polar (0001) and N-polar (000 $\bar{1}$ ). While the intrinsic bulk-terminated GaN(0001) surface is disordered, a series of surface reconstructions can be prepared by putting additional Ga, from the N-rich  $2\times 2$ , [5,6] to the Ga-rich  $4\times 4$ ,  $2\times 2$ ,  $5\times 5$  [7,8],  $4\times 6$  [5] and the most Ga-rich pseudo- $1\times 1$  surface [5–9]. Typical MOCVD and MBE growth of GaN are performed under Ga-rich conditions, and it has been shown that the pseudo- $1\times 1$  surface plays a role of surfactant layer promoting the two dimensional step-flow growth [9,10]. Thus from the practical point of view, the pseudo  $1\times 1$  surface is the first candidate for studying the metal adsorption and growth. Smith et al. [5, 6] have determined that the surface has about 2–3 ML (1ML refers to the atomic density in the GaN(0001) plane, i.e.,  $1.1 \cdot 10^{15} \text{ cm}^{-2}$ ) additional Ga, and it is characterized by a  $\delta$ - $1\times 1$  reflection high-energy electron dif-

fraction (RHEED) pattern. The STM image is usually smooth and featureless, and  $1\times 1$  corrugation can be observed only under specific tunneling condition. A “Ga fluid” model has been proposed by Smith et al. [5, 6] and Northrup et al. [11]. According to this model two additional Ga adlayers above GaN surface are present. The first layer of Ga is fixed in  $1\times 1$  configuration, and the second layer (top layer) has a contracted structure with the Ga density of 1.3ML (similar to some metal surface at high temperature, e.g., Ir [12], Pt [13], and Au [14]). It is very interesting to note that the top layer of Ga is intrinsically mobile at room temperature, resulting in the  $1\times 1$  corrugation observed by the STM. Mula et al. [9] have reported that the pseudo- $1\times 1$  surface is very stable and further deposition of several hundred ML Ga doesn't change the structure, indicating a zero sticking coefficient of Ga on this Ga-saturated surface.

We had chosen the GaN(0001)-pseudo  $1\times 1$ -Ga (hereafter as “Ga-fluid”) surface as the substrate and then studied the adsorption of Au submonolayer at RT. We have found two new reconstructions induced by Au at RT, i.e., the commensurate  $c(2\times 12)$  reconstruction ( $\alpha$ -phase) and incommensurate  $\beta$ -phase. Results of spectra measurements clearly demonstrate a possibility of formation 1D and 2D systems on the basis of a mix Au-Ga adatom structure. All the experiments were performed in ultra high vacuum conditions. The quality of tunneling tips was controlled by field ion microscope (FIM) attached to STM chamber [15]. We used commercial PtIr tips as successfully as tips prepared from the  $\langle 111 \rangle$ -oriented W-crystal wire by electro-chemical etching. Before scanning the tips were degas at 500 °C during 8 hours then field evaporation was used to remove the oxide layers and to shape the scanning tips. The substrate was a commercial 1.5 mm-thick GaN(0001) film grown

<sup>1)</sup>e-mail: oreshkin@spmlab.phys.msu.su

on a SiC(0001) wafer by MOCVD. RHEED was employed to monitor the surface structure during growth. Au was evaporated from a tungsten coil heater, and the Au flux was controlled by the heater current. The typical flux used in the present study was 0.2 ML/min.

Both filled and empty state images were acquired at constant current mode with tunnel bias voltage applied to the sample and tunneling current of 20 pA. The GaN(0001)-pseudo  $1 \times 1$  is formed by terminating MBE growth on the GaN (0001) surface under Ga-rich conditions. Fig.1 shows an STM image of Ga-rich surface (pseudo  $1 \times 1$ ), prepared by deposition about 2 ML of Ga

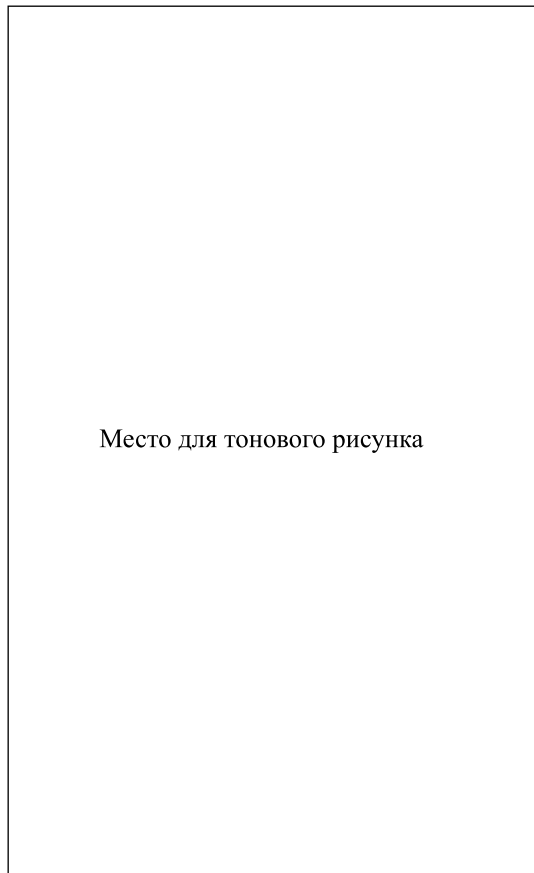
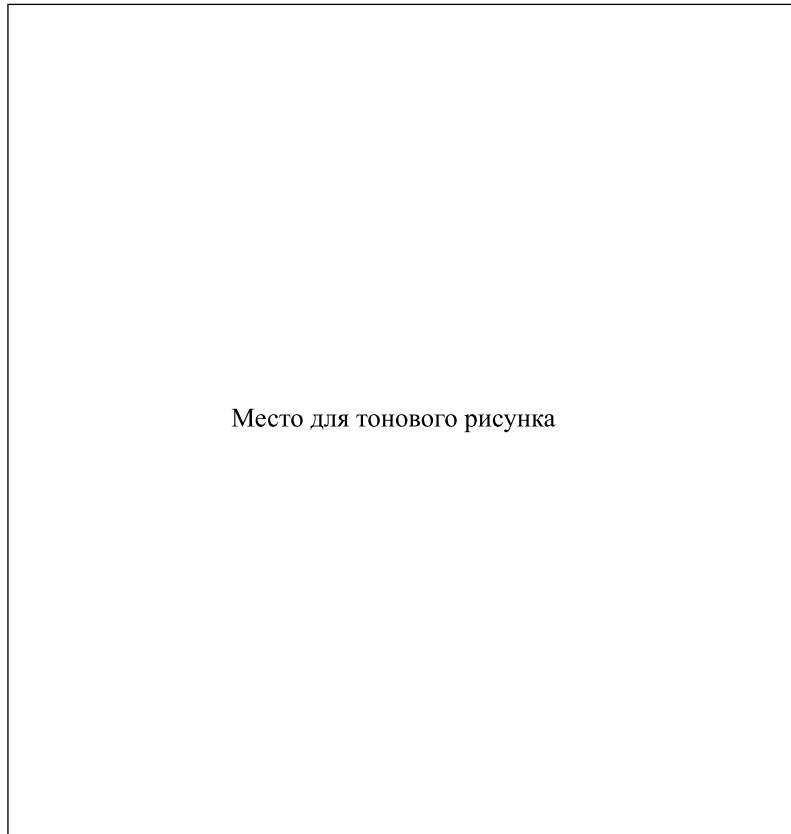


Fig.1. Filled state STM images of (a) as-prepared “Ga fluid” ( $2500 \text{ \AA} \times 2200 \text{ \AA}$ ). At normal tunneling conditions the surface is smooth and without corrugation. The inset image shows a  $40 \text{ \AA} \times 40 \text{ \AA}$  area with  $1 \times 1$  corrugation obtained at a sample bias of  $-0.1 \text{ V}$ . (b) After adsorption of Au at coverage of  $\sim 0.02 \text{ ML}$ , two patches of  $c(2 \times 12)$  ( $\alpha$ -phase) and  $\beta$ -phase form on the same isolated double step-height terrace (about  $1200 \text{ \AA}$  in size)

above the last GaN bilayer. This STM image demonstrates large and smooth terraces with typical terrace width of several hundred  $\text{\AA}$  with no specific features in both filled and empty state STM images. The  $1 \times 1$

atomic corrugation can be observed only with very sharp tip at very low bias voltage, as shown in the inset in Fig.1a. The RHEED pattern of this surface demonstrates “ $1 \times 1$ ” pattern, consistent with STM observation. The presence of the satellite peaks indicates the contraction of the Ga adatom layer, and the  $1 \times 1$  structure observed by STM is due to the mobility of the top Ga adlayer. These observations are consistent with the report by Smith and Northrup [6, 11]. After deposition of Au submonolayer on the pseudo  $1 \times 1$  surface at room temperature we were able to observe two new phases on the surface. There are two reconstructions: commensurate  $c(2 \times 12)$  ( $\alpha$ -phase) and incommensurate  $\beta$ -phase. The area of the two new phases increases with increasing Au coverage until they fully cover the whole surface. Fig.1b shows the simultaneous formation of  $\alpha$ - and  $\beta$ - phases at Au coverage of about 0.02 ML. As can be seen from this image, two patches of  $\alpha$ - and  $\beta$ -phases are formed on the same terrace (double step height) initially covered by “Ga fluid”. The size of the terrace is about  $1000 \text{ \AA}$ . The corrugation height of  $\beta$ -phase is apparently bigger than one for  $\alpha$ -phase (the height profile measurement gives a height difference of  $2.0 \text{ \AA}$  and  $0.5 \text{ \AA}$ , respectively, with respect to the Ga fluid surface). The  $c(2 \times 12)$  reconstruction ( $\alpha$ -phase) (Fig.2a) contains parallel atomic rows running along the  $[11\bar{2}0]$  direction, in which each pair of bright rows is separated by a dark row. The unit cell is rectangular, and the periodicity in the  $[11\bar{2}0]$  and  $[1\bar{1}00]$  directions are  $2a$  and  $6(\sqrt{3}/2)a$ , respectively, which is denoted as  $c(2 \times 12)$  reconstruction. The periodicity can be further confirmed by the RHEED measurement, as shown in Fig.2b. The “ $6 \times$ ” in the  $[11\bar{2}0]$  azimuth and a “ $4 \times$ ” in the  $[1\bar{1}00]$  azimuth are clearly identified, corresponding to a  $c(2 \times 12)$  periodicity in the real space. Another common Au-induced phase is the incommensurate  $\beta$ -phase. Fig.3 shows two STM images of the same place of the  $\beta$ -phase at different bias voltage polarities. The corrugation height is smaller for filled states STM image (Fig.3a) compare to empty states one (Fig.3b). In more details this will be discussed later. The structure consists of hexagonally packed protrusions with the nearest neighbor distance of  $\sim 8.6 \text{ \AA}$ . The closed-packing direction is along the  $[1\bar{1}00]$  direction,  $30^\circ$  rotated from the closed-packing direction of substrate,  $[11\bar{2}0]$ . Ring-like modulation patterns can be observed randomly distributed on the surface. We suggest that the incommensurate  $\beta$ -phase is two-dimensionally grown Au islands, where the underlying Ga bilayer structure still remains. First, the height difference between the  $\beta$ -phase and the “Ga fluid” substrate is about  $2 \text{ \AA}$ , in consistence to the inter layer distance of the Au(111) plane (this is much higher than the



Место для тонового рисунка

Fig.2. (a) Zoom in image of the  $c(2 \times 12)$  reconstruction. The tunneling current is 20 pA at sample bias voltage of 0.4 V, the image scale is  $90 \text{ \AA} \times 70 \text{ \AA}$ . (b) RHEED pattern of the  $c(2 \times 12)$  surface, where  $6 \times$  in the  $[11\bar{2}0]$  and  $4 \times$  in the  $[1\bar{1}00]$  directions are identified. This corresponds to a  $c(2 \times 12)$  periodicity in the real space

$c(2 \times 12)$ -Au phase where the height difference is only about  $0.5 \text{ \AA}$ . Second, the nearest maxima spacing is  $8.6 \text{ \AA}$ , being incommensurate with the substrate lattice constant of  $3.19 \text{ \AA}$ . But it is approximately three times the lattice constant on the Au(111) plane,  $2.88 \text{ \AA}$ . So, this structure can be explained by pure Au(111) islands formed on the top of Ga fluid surface. The  $3 \times$  corrugation is possible strain-induced modulation patterns due to 4% lattice mismatch between Au ( $2.88 \text{ \AA}$ ) and the Ga-fluid ( $2.76 \text{ \AA}$ ), that is much smaller than the mismatch between Au and the bulk GaN substrate (10%). This is the reason why we can prepare flat Au film on the Ga-fluid surface, while the growth of Au on bulk-terminated GaN surface results in 3D agglomerations (the result will be published elsewhere). It should be noted that upon the formation of the  $\beta$ -phase, the originally mobile Ga atoms on the underneath "Ga fluid" substrate have to cease moving. This may result in the segregation of some of the Ga atoms into Au surface, which is a likely origin of the ring-like patterns observed in the STM images. The discovered ring-like structure can be of interest for nanotechnology be-

cause of good reproduction and small scattering parameter.

The I-V characteristics measured above surface area of  $\beta$ - and  $\alpha$ -phases are present on Fig.4. Before these measurements the tip was fixed at certain surface site (ring-like or  $c(2 \times 12)$  structure) with fixed tunneling parameters:  $V_s = -2.0 \text{ V}$ ,  $I_t = 50 \text{ pA}$ . The best STM images of ring-like structure were obtained in the range of  $V_s = \pm 0.5 \text{ V}$ . That is in the good agreement with our STS spectra. As one would expect from Fig.4a the contrast of STM image at  $V_s = +0.5 \text{ V}$  should be higher than this one at  $V_s = -0.5 \text{ V}$ . This difference is clearly seen from Fig.3. It is obvious that spectra have metallic like character. Tunneling conductivity measured above  $c(2 \times 12)$  structure reveal peak at zero bias voltage. Moreover two dips at  $0.25 \text{ V}$  and  $-0.15 \text{ V}$  are clearly seen on normalized tunneling conductivity  $(dI/dV)/(I/V)$  curves. Two peaks also appear on tunneling conductivity curves at  $0.5 \text{ V}$  and  $-0.5 \text{ V}$ . We connect this behavior of tunneling conductivity with quasi one dimensional character of electronic density of states along double-chain structure ( $c(2 \times 12)$ ). The electron

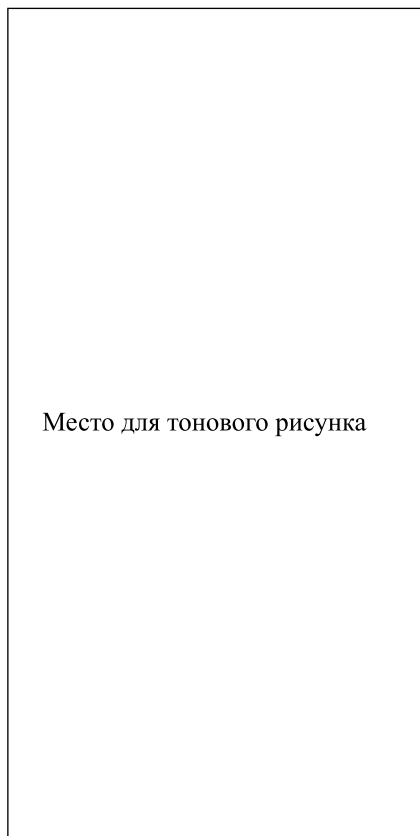


Fig.3. STM image of the same site of  $\beta$ -phase structure ( $175 \text{ \AA} \times 175 \text{ \AA}$ ). The tunneling current is 50 pA (a) Filled state STM image of ring-like structure ( $V = -0.5 \text{ V}$ ). (b) Empty state STM image of ring-like structure ( $V = 0.5 \text{ V}$ )

states of the double-chain structure ( $c(2 \times 12)$ ) can be described by simple model hamiltonian.

$$\hat{H} = \sum_{k,\sigma} \varepsilon_{1k} a_{1k\sigma}^+ a_{1k\sigma} + \varepsilon_{2k} a_{2k\sigma}^+ a_{2k\sigma} + T a_{1k\sigma}^+ a_{2k\sigma} + \text{h.c.} \quad (1)$$

Where  $\varepsilon_{1k} = \varepsilon_{2k} = t \cos(ka)$  1D energy spectrum of electrons along each noninteracting chain;  $t$  – hopping matrix element between nearest neighbouring sites along each chain of  $c(2 \times 12)$  structure.  $a_{ik\sigma}^+$  ( $a_{ik\sigma}$ ) – creation (annihilation) operator of electron in state with momentum  $k$  and spin  $\sigma$  in the  $i$ -th chain ( $i = 1, 2$ ). The last term in the Hamiltonian corresponds to the interaction between nearest neighbours in different chains with hopping matrix element  $T$ . In  $k$ -space the exact retarded electron Green function along each chain can be easily obtained. For example:

$$G_{kk}^1 = \frac{\omega - \varepsilon_{2k}}{(\omega - \varepsilon_{1k})(\omega - \varepsilon_{2k}) - T^2}. \quad (2)$$

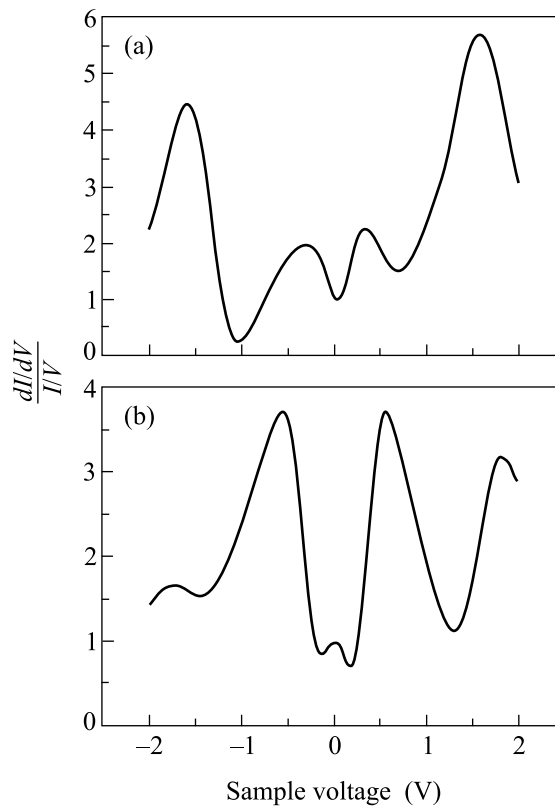


Fig.4. Normalized tunneling conductivity measured above: (a) ring-like structure, (b)  $c(2 \times 12)$  structure

The poles of Green functions determine the electronic spectrum of double-chain structure:

$$\omega_{\pm} = t \cos(ka) \pm T. \quad (3)$$

The density of states along each of interacting chains can be obtained as:

$$-\frac{1}{\pi} \text{Sp}_k \text{Im}(G_{kk}^{1(2)}(\omega)) = \nu_{1(2)}(\omega). \quad (4)$$

So, we have two splitted quasi 1D bands which are centered at  $\pm T$  and have the width  $2t$ . In symmetric case one can obtain splitted bands and 1D character of density of states:

$$\nu_{1(2)}(\omega) = \frac{1}{2ta} \left( 1 - \left( \frac{\omega - T}{t} \right)^2 \right)^{-1/2} + \frac{1}{2ta} \left( 1 - \left( \frac{\omega + T}{t} \right)^2 \right)^{-1/2}. \quad (5)$$

It is reasonable to assume that  $T$  and  $t$  are comparable because the distance between the chains is just the same as interatomic distance along the chain. So one can expect the appearance of two deeps in the tunneling conductivity spectra when the value of applied bias

approaches the energy center of each splitted 1D band:  $eV = \pm T$ . When applied voltage  $eV$  is close to the energy values of band edges:  $eV = -T \pm t$  or  $eV = T \pm t$ , one should obtain strongly increased tunneling conductivity, because 1D density of states has power law singularity at band edges with power law exponent  $-\frac{1}{2}$ . Similar dependence of local tunneling conductivity versus applied bias voltage is observed near double-chain structure during STS measurements is shown on Fig.4b. Singularities in tunneling conductivity are smoothed by interaction with substrate, but peaks in  $(dI/dV)/(I/V)$  curves, corresponding to the edges of each 1D splitted bands are clearly seen at zero applied bias and at  $V = 0.5$  V and  $V = -0.5$  V. Two dips are also present at  $(dI/dV)/(I/V)$  curves at applied bias  $V = 0.25$  V and  $V = -0.15$  V. In contrary to the  $c(2 \times 12)$  structure the tunneling conductivity above ring-like surface structure has no features of quasi 1D density of states. The tunneling conductivity peak at zero applied bias voltage is absent: a dip is clearly seen at  $eV = 0$  on  $(dI/dV)/(I/V)$  curves. Two peaks for ring-like structure instead of dips for  $c(2 \times 12)$  structure when the applied bias voltage is 0.2 V and  $-0.2$  V have been found. Such behaviour of local tunneling conductivity especially the dip at small bias voltage should be connected with disordered two-dimensional surface structure in  $\beta$ -phase.

In conclusion, two new reconstructions on the GaN(0001)-pseudo  $1 \times 1$ -Ga surface induced by Au at RT (i.e., the commensurate  $c(2 \times 12)$  reconstruction ( $\alpha$ -phase) and incommensurate  $\beta$ -phase) have been found. Scanning tunneling spectroscopy measurements revealed the existence of ordered one dimensional structure with specific features in tunneling conductivity spectra as well as disordered two dimensional ring-like structure on the basis of GaN(0001)-pseudo  $1 \times 1$ -Ga surface.

This work was partially supported by SAS # 30/03-MC, project # 1604.2003.2, RFBR # 03-02-16807 and "Nanostructures"-7. We gratefully acknowledge T. Sakurai for valuable discussions.

- 
1. S. Nakamura, T. Mukain, and M. Senoh, Appl. Phys. Lett. **64**, 1687 (1994).
  2. F. A. Ponce and D. A. Bour, Nature **386**, 351 (1997).
  3. S. Nakamura and G. Fasol, *The Blue Laser Diodes (GaN Based Light Emitters and Lasers)*, B.Heidelberg: Springer, 1997, p. 175.
  4. J. I. Pankove, M. Leksono, S. S. Chang et al., MRS-Internet-NSR **1**, 39 (1997).
  5. A. R. Smith, R. M. Feenstra, D. W. Greve et al., Surf. Sci. **423**, 70 (1999).
  6. A. R. Smith, R. M. Feenstra, D. W. Greve et al., J. Vac. Sci. Technol. **B16**, 2242 (1998).
  7. Q. K. Xue, Q. Z. Xue, R. Z. Bakhtizin et al., Phys. Rev. Lett. **82**, 3074 (1999).
  8. Q. Z. Xue, Q. K. Xue, R. Z. Bakhtizin et al., Phys. Rev. **B59**, 12604 (1999).
  9. G. Mula, C. Adelmann, S. Moehl et al., Phys. Rev. **B64**, 195406 (2001).
  10. L. X. Zheng, M. H. Xie, S. M. Seutter et al., Phys. Rev. Lett. **85**, 2352 (2000).
  11. J. E. Northrup, J. Neugebauer, R. M. Feenstra, and A. R. Smith, Phys. Rev. **B61**, 9932 (2000).
  12. M. A. Van Hove, R. J. Koestner, P. C. Stair et al, Surf. Sci. **103**, 189 (1981).
  13. U. Harten, A. M. Lahee, J. P. Toennies, and Ch. Woll, Phys. Rev. Lett. **54**, 2619 (1985).
  14. A. R. Sandy, S. G. J. Mochrie, D. M. Zehner et al., Phys. Rev. Lett. **68**, 2192 (1992).
  15. T. Sakurai et al., Prog. Surf. Sci. **33**, 3 (1990).